Genomics

Molecular Cancer Research

Multigene Profiling of CTCs in mCRPC Identifies a Clinically Relevant Prognostic Signature

Udit Singhal[1], Yugang Wang[1], James Henderson[1], Yashar S. Niknafs[2], Yuanyuan Qiao[3], Amy Gursky[1], Alexander Zaslavsky[1], Jae-Seung Chung[1,4], David C. Smith[5], R. Jeffrey Karnes[6], S. Laura Chang[7], Felix Y. Feng[7], Ganesh S. Palapattu[1,8], Russell S. Taichman[9], Arul M. Chinnaiyan[10], Scott A. Tomlins[11], and Todd M. Morgan[1]

Abstract

The trend toward precision-based therapeutic approaches dictated by molecular alterations offers substantial promise for men with metastatic castration-resistant prostate cancer (mCRPC). However, current approaches for molecular characterization are primarily tissue based, necessitating serial biopsies to understand changes over time and are limited by the challenges inherent to extracting genomic material from predominantly bone metastases. Therefore, a circulating tumor cell (CTC)-based assay was developed to determine gene expression across a panel of clinically relevant and potentially actionable prostate cancer–related genes. CTCs were isolated from the whole blood of mCRPC patients ($n = 41$) and multiplex qPCR was performed to evaluate expression of prostate cancer–related target genes ($n = 78$). A large fraction of patients (27/41, 66%) had detectable CTCs. Increased androgen receptor (*AR*) expression (70% of samples) and evidence of Wnt signaling (67% of samples) were observed. The *TMPRSS2:ERG* fusion was expressed in 41% of samples, and the aggressive prostate cancer–associated long noncoding RNA *SChLAP1* was upregulated in 70%. *WNT5a* [HR 3.62, 95% confidence interval (CI), 1.63–8.05, $P = 0.002$], *AURKA* (HR 5.56, 95% CI, 1.79–17.20, $P = 0.003$), and *BMP7* (HR 3.86, 95% CI, 1.60–9.32, $P = 0.003$) were independently predictive of overall survival (FDR < 10%) after adjusting for a panel of previously established prognostic variables in mCRPC (Halabi nomogram). A model including Halabi, *WNT5a*, and *AURKA* expression, termed the miCTC score, outperformed the Halabi nomogram alone (AUC = 0.89 vs. AUC = 0.70). Understanding the molecular landscape of CTCs has utility in predicting clinical outcomes in patients with aggressive prostate cancer and provides an additional tool in the arsenal of precision-based therapeutic approaches in oncology.

Implications: Analysis of CTC gene expression reveals a clinically prognostic "liquid biopsy" signature in patients with metastatic castrate-resistance prostate cancer. *Mol Cancer Res; 16(4); 643–54.* ©2018 AACR.

Introduction

Prostate cancer is the most common cancer diagnosis and the second leading cause of cancer-related deaths among men in the United States (1). While most patients harbor indolent versions of the disease, a large subset experience metastatic progression, recurrence, and resistance to therapy. Although the androgen signaling pathway is the most common driver of prostate cancer disease progression, a number of other genes and pathways have been recognized as potential prognostic markers and therapeutic targets, and after an initial response to androgen deprivation, metastatic prostate cancer will often progress to castrate-resistant disease (mCRPC; refs. 2–8).

Multiple adaptive mechanisms have been delineated that combat pharmacologic androgen starvation in men with mCRPC, including androgen receptor (*AR*) amplification, splicing, and mutation, or initiation of parallel androgen synthesis and proliferative pathways (9–11). Wnt signaling is one such pathway that has been implicated as a downstream mediator of AR signaling in mCRPC, and it has been suggested that AR-regulated noncanonical Wnt signals promote prostatic tumor growth, the development of osteoblastic metastasis, prostate cancer stem cell self-renewal and proliferation, and resistance to antiandrogen therapy (12–16).

Through extensive tissue-based sequencing, it is now clear that prostate cancers harbor diverse, clinically actionable drivers of

[1]Department of Urology, University of Michigan, Ann Arbor, Michigan. [2]Michigan Center for Translational Pathology, University of Michigan, Ann Arbor, Michigan. [3]Michigan Center for Translational Pathology, Department of Pathology, Comprehensive Cancer Center, University of Michigan, Ann Arbor, Michigan. [4]Department of Urology, Inje University, Haeundae Paik Hospital, Busan, Korea. [5]Department of Hematology/Oncology, Department of Urology, University of Michigan, Ann Arbor, Michigan. [6]Department of Urology, Mayo Clinic, Rochester, Minnesota. [7]Department of Radiation Oncology, Helen Diller Comprehensive Cancer Center, University of California at San Francisco, San Francisco, California. [8]Department of Urology, Medical University of Vienna, Vienna, Austria. [9]Department of Periodontics and Oral Medicine, University of Michigan School of Dentistry, University of Michigan, Ann Arbor, Michigan. [10]Michigan Center for Translational Pathology, Department of Pathology, Comprehensive Cancer Center, Howard Hughes Medical Institute, University of Michigan, Ann Arbor, Michigan. [11]Departments of Pathology and Urology, Comprehensive Cancer Center, Michigan Center for Translational Pathology, University of Michigan, Ann Arbor, Michigan.

Note: Supplementary data for this article are available at Molecular Cancer Research Online (http://mcr.aacrjournals.org/).

U. Singhal and Y. Wang contributed equally to this article.

Corresponding Author: Todd M. Morgan, University of Michigan, Ann Arbor, 1500 East Medical Center Drive, 7308 CCC, Ann Arbor, MI 48109-5946. Phone: 734-615-6662; Fax: 734-615-6662; E-mail: tomorgan@med.umich.edu

doi: 10.1158/1541-7786.MCR-17-0539

disease progression that may inform both prognosis and potential response to therapy (4, 17–19). While these findings highlight the promise of precision oncology testing in prostate cancer, the utility of these techniques may be limited by both the challenges of extracting viable tissue from bone metastases and the need for serial sampling as new resistance mechanisms arise (18, 20).

Emerging comprehension in the realm of circulating tumor cell (CTC) biology has unveiled the potential for noninvasive, continuous monitoring of cancer, and previous studies have established a correlation between CTC, primary tumor, and metastatic tissue gene expression profiles (21, 22). Previous efforts to inform disease severity in prostate cancer have relied simply on the presence or absence of CTCs, but these studies have not yielded adequate clinical utility to guide therapeutic decision-making for individual patients (23–26). Additionally, genomic profiling of cell-free DNA (cfDNA) represents another feasible and clinically informative liquid biopsy avenue in mCRPC (27, 28). While newly developed approaches show promise in CTC detection, including CTC-iChip and the AdnaTest, the overall landscape of liquid approaches to assess changes in tumor behavior in men with mCRPC represents a major unmet clinical need as robust, readily reproducible methods for isolation and subsequent characterization of CTCs in prostate cancer remain elusive (9, 29, 30).

To facilitate noninvasive detection of genomic alterations and molecular expression in these patients, we developed and implemented a qPCR-based platform for analysis of CTCs from men with mCRPC. This approach was modeled after commercially available, tissue-based qPCR platforms for prostate cancer profiling, with the primary goal of eventual integration into clinical workflows (31, 32). Given that CTCs likely represent cells from disparate metastatic sites, we hypothesized that understanding the expression of key genes of interest within CTCs could have unique utility in precision medicine approaches to predict clinical outcomes in patients with advanced prostate cancer (33).

Materials and Methods

CTC isolation, gene expression determination, and platform validation

CTCs were isolated from 5-mL whole blood using anti-EpCAM antibody–conjugated microbeads (Thermo Fisher Scientific). *DAPI*, *CD45*, *FITC*, and PCa-CT-PE (antibody cocktail: *PSMA*, *EGFR*, and pan-cytokeratin) were used to confirm the identity of CTCs. Following washing and cell lysis, mRNA from CTCs was captured using Oligo(dT)25 mRNA Dynabeads (Thermo Fisher Scientific). Reverse transcription was performed to obtain cDNA, followed by preamplification to generate target gene amplified libraries, and multiplex qPCR was then performed to evaluate a panel of 96 genes, including controls (Supplementary Table S1). Genes were selected based on relevance to prostate cancer progression and metastasis, as well as EMT and cancer stem cell biology. To account for leukocyte contamination, blood processed from 27 healthy controls was used as a baseline referent. To evaluate gene amplification efficiency for both preamplification and real-time PCR, prostate cancer cells (1.65×10^4 cells, including equal amount of PC3, VCaP, and LNCaP) were lysed with 1 mL lysis buffer. Ten-fold serial dilution was applied with lysis buffer to obtain samples equal to 3,300, 330, 33, 3.3, and 0.33 cells per 200 uL to evaluate the linear relationship between cell number and cycle threshold (Ct) value of individual genes (Supplementary Fig. S1). To further validate the RT and amplification steps, we included Array control RNA Spikes (Thermo Fisher AM1780), using primers from the Fluidigm RNA Spikes Assay kit (100-5582) to validate the reverse transcription, preamplification, and qPCR steps. The kit contains RNA from *E. coli* with no known homology to mammalian sequences. Spike mix was prepared as described in the Fluidigm delta gene assay protocol, PN 100-4904 J1. Three of the RNA spikes were used, Spike-1 (750 nucleotides), Spike-4 (1000 nucleotides), and Spike-7 (1474 nucleotides) and mixed. Ct value of each RNA spike was acquired with qPCR. The average value plus standard deviation of Ct value from different spikes was calculated and plotted against the copy number of different spikes, which showed a linear correlation between Ct value and copy number ($R^2 = 0.95$; Supplementary Fig. S1).

For platform validation, 180 GFP-labeled prostate cancer cells (PC3, LNCaP, and VCaP) were sorted into 5-mL whole blood from a normal donor. Cells were captured using immunomagnetic bead enrichment and visualized by immunofluorescence. Cells were then counted, rather than lysed, to measure the recovery rate. Additionally, 300 PC3 and LNCaP cells were spiked into 5 mL of whole blood from healthy controls and captured by immunomagnetic bead enrichment, followed by staining with *DAPI*, *CD45*, and PCa-CT (antibody cocktail: *PSMA*, *EGFR*, and pan-cytokeratin) to visualize CTCs. To validate gene expression after CTC isolation, 10 prostate cancer cells (PC3, LNCaP, or VCaP) were spiked into 5 mL of whole blood from a normal control. CTCs were captured by immunomagnetic bead enrichment, lysed, and gene expression was then assessed by qPCR. qPCR gene expression was compared with known microarray profiles for each of these lines in order to evaluate whether the expression profiles matched that of what was expected for PC3, LNCaP, and VCaP cells.

Normalization of qPCR gene expression data

For each sample, gene expression of 96 genes was determined from qPCR in a 384-well format as described above. Ct values were normalized using the ΔΔCt method as previously described (34). Briefly, genes within each sample were first normalized against endogenous controls by subtracting the sample-specific average Ct value for *ACTB*, *HMBS*, and *TUBA-1B*. For each gene, the resulting ΔCt values were corrected for background from contaminating blood cells by subtracting the average ΔCt value for that gene across the 27 healthy donor reference controls to obtain ΔΔCt values. Undetermined Ct values were imputed as 40 (Supplementary Table S2). Finally, gene expression was quantified as $2^{-\Delta\Delta Ct}$, which we refer to as "normalized expression." All analyses were performed with $\log_2$(normalized expression + 1), with the logarithm serving as a variance-stabilizing transformation and the addition of the constant serving to compress expression values comparable to background. In addition, we set gene expression values to zero when the underlying Ct value was greater than 35 as Ct values in this range are generally not quantifiable.

Classification of samples as CTC positive or negative

Given that this protocol involves cell lysis rather than visualization and enumeration, we established a model for identifying CTCs using the gene expression of eight epithelial markers: *CD326*, *CDH1*, *CDH2*, *DSG2*, *EGFR*, *KRT8*, *KRT18*, and *KRT19*. CTC-positive controls were created using serial dilutions of prostate cancer cell lines, PC3 and LNCaP, spiked into whole blood from healthy donors. Data from 27 healthy donor controls were

used as negative controls. We first performed a principal components analysis to verify the accuracy of these genes for distinguishing positive from negative controls. The first principal component clearly separates positive from negative controls, with the second component primarily separating cell lines (Supplementary Fig. S2). These two components account for 92% and 4% of variance for these samples, respectively. The weights of each gene on this component are shown as a bar graph in Supplementary Fig. S2. We define an epithelial score (ES) as the weighted sum of the eight epithelial marker genes using these weights. We then built a classification model for identifying new samples with CTCs using this epithelial score in a logistic regression. The fitted model is:

$$\mathrm{P}(\text{CTCs present} \mid \text{gene expression}) = \exp(\mathrm{a} + \mathrm{b} \times \mathrm{ES})/(1 + \exp(\mathrm{a} + \mathrm{b} \times \mathrm{ES})), \mathrm{a} = -7.80, \mathrm{b} = 0.94$$

Patient samples were considered CTC positive if they are above the conservative threshold of 75% on the estimated probability using the model above. In both the control and clinical settings, the majority of samples were toward the very high or very low end of the CTC probability model (Supplementary Fig. S2).

Cox proportional-hazard survival models

The primary endpoint for this study was overall survival, and in order to identify CTC-based genes associated with mortality, we performed univariate Cox regression analysis in CTC-positive patients for each of the measured genes (35). The Halabi nomogram was utilized to account for baseline clinicopathologic variables, including ECOG performance status, disease site, opioid analgesic use, albumin, hemoglobin, alkaline phosphatase, and PSA in a multivariate Cox model. We obtained 18-month survival probabilities from https://www.cancer.duke.edu/Nomogram/firstlinechemotherapy.html. We subtract this probability from one to define a "Halabi" score so that hazard ratios above one indicate increased risk of death. Cox bivariate regression analyses were then performed for each gene, adjusting for Halabi score, to identify genes associated with mortality independent of measureable clinical factors.

Cox regression was performed for 78 genes, after removing endogenous controls (*ACTB*, *HMBS*, and *TUBA-1B*), epithelial markers (*CD326*, *CDH1*, *CDH2*, *DSG2*, *EGFR*, *KRT8*, *KRT18*, and *KRT19*), blood-cell markers (*CD20* and *CD45*), artificial RNAs used in assay development (Spike1, Spike4, and Spike7), and alternate primers for *SChLAP1* and *SPANXB2*. Log-transformed normalized expression values for each gene were rescaled by the interquartile range in order to make hazard ratios easier to interpret. Models were fit using the R function *coxph* in the *survival* package (36). Genes were ranked using *P* values from bivariate proportional hazards models with a single gene and the Halabi score as predictors. These *P* values were transformed to FDR q-values using the Benjamini–Hochberg method (37). The three genes significant at <10% FDR in the CTC-positive cohort—*AURKA*, *BMP7*, and *WNT5A*—were selected for further analysis. Cox regression and Kaplan–Meier analysis was performed to assess whether CTC-positive or -negative status was associated with survival within the cohort. To aid in the interpretation of hazard ratios, we repeated the analysis using CTC probability based on our epithelial score as a continuous variable. This probability "*P*" was scaled using the transform: $2 \times (P - 0.5)$, so that one unit change can be thought of as going from $P = 0.25$ to $P = 0.75$.

Determining prognostic potential of selected genes

We constructed waterfall plots based on expression of WNT5a, AURKA, and BMP7 for the 39 patients (26 CTC positive) with at least 6-month follow-up with bars colored by vital status at 6 months. In these plots, patients in the CTC-positive subgroup were ordered from lowest to highest normalized expression and patients without CTCs ordered below the CTC-positive group. To assess significance in these plots, we used the hypergeometric distribution to test whether deaths were overrepresented in the top 25% of patients.

We next examined composite scores using these three genes. First, in the CTC-positive group we assigned patients points for each gene, with normalized expression values in the 50th to 75th percentiles given one point, and those above the 75th percentile given two points. Then, we defined prognostic scores by adding point values across either all three genes or one of the three two-gene pairs. For these four scores, we constructed receiver operating characteristic (ROC) curves for predicting vital status at 6 months using the *survivalROC* function with smoothing parameter lambda = 0.002 from the *survivalROC* package in R (38, 39).

From the ROC analysis, we identified the best performing genes (*WNT5a* and *AURKA*) and added those to the Halabi score to generate a combined molecular and clinical signature. The resulting miCTC score ranges continuously from 0 to 5, with integer values of 0, 1, 2, 3 or 4 coming from AURKA and WNT5A gene expression. We use 1 minus the Halabi 18-month survival probability as the "Halabi component" of the score. As before, we use the *survivalROC* function in R to construct ROC curves for predicting survival at 6 months (180 days) using the miCTC and Halabi scores. Confidence intervals for the difference in AUCs between these two curves were computed using the appropriate quantiles from 10,000 bootstrap samples. Finally, we define a "high-risk" subgroup as those patients having a miCTC score of two or more, with others forming a "low-risk" subgroup. We compare these risk groups using Kaplan–Meier survival curves and assess significance using the log-rank test. Survival curves and log-rank *P* values are computed using the *survfit* and *survdiff* functions from the *survival* package (40).

Survival analysis

Formalin-fixed paraffin-embedded prostatectomy samples were from two published retrospective patient cohorts from the Mayo Clinic ($n = 780$; refs. 41–43). As previously described, RNA extraction and hybridization to Affymetrix Human Exon 1.0 ST Arrays (Affymetrix) were performed in a CLIA-certified, clinical operations laboratory (GenomeDx Biosciences, Inc.). Microarrays were normalized using Single Channel Array Normalization (44). Microarray data are available with NCBI GEO accession numbers GSE46691 and GSE62116. The miCTC score was applied to the retrospective samples as described above. Kaplan–Meier curves were generated for the pooled Mayo Clinic cohorts, and hazard ratio estimates were generated using Cox proportional hazards modeling.

All cell lines were obtained from the ATCC, and cell lines were maintained using standard conditions. To ensure identity, all cell lines were genotyped at the University of Michigan Sequencing Core using Profiler Plus (Applied Biosystems) and compared with profiles of respective cell lines available from ATCC. Cell authentication and mycoplasma testing was performed for all cell lines. This study was approved by the Institutional Review Board (IRB# HUM00052405), and written informed consent was obtained

from all patients for collection and analysis of samples in accordance with recognized Declaration of Helsinki guidelines.

Results

Development of CTC isolation and gene expression analysis platform

CTC isolation and subsequent gene expression analysis was conducted using an antiepithelial cell adhesion molecule (*EpCAM*)-coated microbead protocol, followed by multiplex qPCR of 78 prostate cancer–related genes plus internal controls (Supplementary Fig. S3). Our panel contained genes previously shown to be involved in prostate cancer aggressiveness, metastasis, or progression, including *TMPRSS2:ERG*, *PSA*, *AR*, *WNT5a*, *NKX3.1*, *EGFR*, and *SChLAP1* (16, 45–49). Recovered cells were identified by cell surface staining for *EpCAM* and absent staining for *CD45*, a common leukocyte marker (50). In order to assess the performance of this platform, small numbers of cells ($n = 10$) were spiked into 5 mL of whole blood. Gene expression analysis of these cells showed expression profiles that were congruent with previous microarray analyses of these cell lines, supporting the validity of our isolation and expression analytic platform (Supplementary Fig. S4).

Isolation and analysis of CTCs from whole blood of patients with mCRPC

To characterize the CTC gene expression pattern in patients, we evaluated 41 patients with mCRPC (Table 1). The median age was 68 (IQR 61–75) and median PSA was 19.7 ng/mL (IQR 3.6–70.6 ng/mL). At the time of enrollment, all patients were on luteinizing hormone releasing hormone (LHRH) agonist therapy (leuprolide and goserelin), 5 patients were on additional treatment with abiraterone, 11 on enzalutamide, 8 on docetaxel, 4 on cabazitaxel, 1 on radium 223, and 1 on dexamethasone. Patients had received a median of two prior therapies (IQR 1–3). All patients had a minimum of 90 days follow-up and there were 21 (51.2%) deaths. The median time to next therapy was 251 days (IQR 119–329) and patients received a median of one subsequent therapy (IQR 0–1).

CTC positivity was determined based on a model using the gene expression of eight epithelial markers (Supplementary Fig. S2) and we identified 27 (66%) patient samples with detectable CTCs. In our protocol, CTC-positive samples are identified after expression profiling, and each profile is potentially a mixture of CTC targets and contaminating blood cells, as this is an enrichment rather than pure isolation approach. For the healthy controls, due to the absence of epithelial CTCs, all RNA in the sequence library is from contaminating blood cells. As described in Materials and Methods, gene expression in patient samples is normalized to both endogenous controls and then to expression in healthy controls to account for background contamination. In order to define potential thresholds regarding positive or negative expression of a given gene in CTCs, we used *k*-means clustering for each gene to find subgroups among 27 healthy controls and 27 CTC-positive samples. When the composition of these two groups was such that one had significantly more CTC-positive samples than healthy controls (as determined by a χ^2 test), we used the midpoint between the cluster means to define a threshold at which to call specific samples "positive" for a given gene. Using this approach, 19 samples (70%) showed increased expression of *AR* and 15 (55%) showed significant expression of *AR-V7*, with 14 (52%) shared between these two groups. Increased downstream *AR* signaling was seen in 14 (52%) samples based on

Table 1. Demographics and baseline characteristics of the mCRPC patient cohort

	Overall, n (%)	CTC positive, n (%)	CTC negative, n (%)	
Variable				
All	43	27 (63)	16 (37)	*P*
Age[a]	68 (61–75)	64 (59–74)	71 (68–75)	0.943
Race				0.537
Caucasian	41 (96)	25 (92)	16 (100)	
African American	1 (2)	1 (4)	0 (0)	
Hispanic	1 (2)	1 (4)	0 (0)	
ECOG PS				0.235
0	18 (42)	9 (33)	9 (56)	
1	23 (53)	16 (59)	7 (44)	
2	2 (5)	2 (8)	0 (0)	
Metastatic site				
Bone	29 (67)	18 (67)	11 (69)	
Visceral	9 (21)	6 (22)	3 (19)	
Regional LN	21 (49)	12 (44)	9 (56)	
Distant LN	4 (9)	3 (11)	1 (6)	
No. of metastatic sites				0.2714
1	15 (35)	9 (33)	6 (38)	
2	16 (37)	9 (33)	7 (44)	
3	11 (26)	8 (30)	3 (19)	
4+	1 (2)	1 (4)	0 (0)	
Prior local therapy				0.1829
Surgery	17 (40)	11 (26)	6 (38)	
Radiation	11 (26)	8 (30)	3 (19)	
Opioid analgesic use	18 (42)	16 (59)	2 (13)	0.001
Albumin[a]	4.1 (3.8–4.3)	4.1 (3.8–4.3)	4.1 (3.95–4.3)	0.769
Hemoglobin[a]	12.55 (11.1–13.0)	12.5 (10.4–13.2)	12.6 (11.95–13.25)	0.898
Alkaline phosphatase[+]	103 (78.5–183)	153 (84–209)	85.5 (72.5–105)	0.008
PSA[a]	19.75 (3.55–70.6)	31.2 (4.7–100.5)	12.45 (12.1–32.1)	0.101

[a]Median value (IQR).

joint expression of *KLK2* (*PSA*) and *NKX3-1*, and 18 (67%) samples showed significant upregulation of Wnt signaling based on expression of *WNT5a*, *WNT5b*, and *BMP7*. Among epithelial–mesenchymal transition (EMT) genes, 9 samples (33%) expressed *SOX2* and 21 (67%) had elevated levels of *TWIST1*, with 7 samples (26%) expressing both genes. Similarly, clustering jointly on *MDK* and *CCNA2*, 15 samples (56%) showed high levels of cell cycle activity. Among long noncoding RNAs (lncRNA) associated with prostate cancer, 19 samples (70%) showed elevated levels of the lncRNA *SChLAP1*, but only 8 (30%) showed increased *PCA3* levels. The *TMPRSS2:ERG* gene fusion was significantly expressed in 11 samples (41%) and based on concordant expression across two distinct amplicons, evidence for the *TM2:ETV1* fusion was seen in 4 samples (15%; Fig. 1A).

To acquire a clinically relevant gene signature, we sought to identify genes expressed in CTCs independently associated with survival. To do this, we performed univariable and multivariable Cox regression analyses of individual genes and used a previously validated prognostic model to account for baseline clinicopathologic variables in mCRPC (51). Increased expression of *WNT5a* (HR 3.62, 95% CI, 1.63–8.05, $P = 0.002$), *AURKA* (HR 5.56, 95% CI, 1.79–17.20, $P = 0.003$), and *BMP7* (HR 3.86, 95% CI, 1.60–9.32, $P = 0.003$) were strongly associated with earlier mortality (FDR < 10%) after adjusting for the Halabi nomogram score. Other genes implicated in prostate cancer biology, including *WNT5b*, *KLK2*, and *PSA*, were significantly associated with overall survival on univariate, but not multivariate, analysis (Fig. 1B). CTC positive or negative status alone was not significantly associated with survival in a Kaplan–Meir analysis ($P = 0.143$) or univariate Cox model (HR 1.9, 95% CI, 0.6–5.7, $P = 0.28$) comparing the two groups. CTC status was also not significantly associated with survival in a bivariate model controlling for Halabi 18-month survival probability (HR 1.2, 95% CI, 0.3–4.0, $P = 0.81$). We repeated this analysis using the CTC epithelial score as a continuous variable, and it was marginally significant in the univariate analysis (HR 3.4, 95% CI, 1.0–11.9, $P = 0.06$) but not the bivariate model adjusted for Halabi 18-month survival probability (HR 2.1 95% CI, 0.5–8.5, $P = 0.28$; Supplementary Fig. S5).

Development of a CTC-based prognostic score

Given the ability of *WNT5a*, *AURKA*, and *BMP7* expression to independently predict survival in this cohort and their previously elucidated roles in metastatic, variant forms of prostate cancer and treatment resistance, we hypothesized that increased expression of these genes within CTCs would correlate with worse prognosis (16, 52–54). Focusing on these three genes, we confirmed that early mortality ($\leq$6 months) occurred more frequently in patients with higher expression of *WNT5a*, *AURKA*, and/or *BMP7* individually (Fig. 2A). We next developed prognostic models in the 27 CTC-positive patients using composite scores for all three genes and evaluated individual combinations of genes to optimize the model. Scores were determined by normalizing the expression values for each gene. One point was given for expression of a given gene in the 50th to 75th percentiles of the CTC cohort and two points for expression above the 75th percentile. While all three genes were individually prognostic, a composite score comprising *WNT5a* and *AURKA* expression outperformed all other combinations (AUC = 0.91; Fig. 2B).

These data were then used to derive a CTC-based prognostic score [hereafter referred to the Michigan CTC (miCTC) score]. This score ranges from 0 to 5, with values of 0, 1, 2, 3, or 4 derived from *AURKA* and *WNT5A* gene expression (0–2 points for expression of each gene as described above). In order to account for baseline clinical variables, the Halabi nomogram score was incorporated as the fifth component into the overall score using the 18-month survival probabilities calculated from the Halabi nomogram (see Materials and Methods; Supplementary Fig. S6). For CTC-negative patients, this meant the miCTC score was based solely on the Halabi survival probability and the absence of *WNT5A* or *AURKA* gene expression. The miCTC score outperformed the Halabi nomogram alone (AUC = 0.89 vs. AUC = 0.70) across the entire 41 patient cohort (Fig. 2C). When categorizing the present cohort into high-risk (miCTC $\geq$ 2) versus low-risk (miCTC <2) subgroups, Kaplan–Meier analysis demonstrated significant differences in overall survival over time (Fig. 2D).

External application of miCTC score using known sequencing data from prostate cancer tissue

To further assess the performance of the miCTC prognostic signature, we first evaluated the level of concordance of gene expression between our qPCR-based platform and tissue-based RNA-sequencing data for a subset of patients enrolled in an ongoing mCRPC profiling study (55). In the 7 patients with both CTC-based qPCR and tissue-based RNA-seq data, a significant level of correlation existed among CTC-to-tissue gene expression (Spearman correlation = 0.38, $P = 0.0002$), suggesting the genomic data obtained from CTCs accurately reflected tissue-based disease (Fig. 3A and B). We then queried the tissue-based expression of *WNT5a* and *AURKA* across a larger database containing samples from normal prostate tissue, localized prostate cancer, and metastatic samples to globally understand the landscape of *WNT5a* and *AURKA* expression (18, 56). As expected, *WNT5a* and *AURKA* expression was found to be significantly upregulated in metastatic samples compared with normal prostate or localized prostate cancer tissue, further supporting the relevancy of these genes in mCRPC (Fig. 3C). Calculation of the miCTC score (using gene expression only) in this cohort revealed a significantly increased proportion of samples with high-risk scores (miCTC $\geq$2) in the metastatic group (92%) compared with the primary cancer group (52%; $P <$ 0.001; Fig. 3D).

miCTC score predicts long-term clinical outcomes in high-risk prostate cancer

Lastly, we applied the gene expression component of the miCTC score to a previously published radical prostatectomy cohort in order to assess its ability to predict long-term, objective outcomes in patients with high-risk, clinically localized prostate cancer (41–43). This cohort included 780 patients with a median follow-up of 11.2 years after prostatectomy. A total of 513 patients (65.8%) suffered biochemical recurrence following prostatectomy, 288 (36.9%) developed metastatic disease, 166 (21.3%) died of their disease, and 336 (43.1%) died of any cause. *WNT5a* and *AURKA* expression were determined from the genomic data and used to calculate the miCTC score (on a scale of 0–4 without the additional factor of the Halabi score). These scores were then matched with clinical outcomes. As shown in the Kaplan–Meir analyses, high-risk and increasing miCTC scores were associated

A

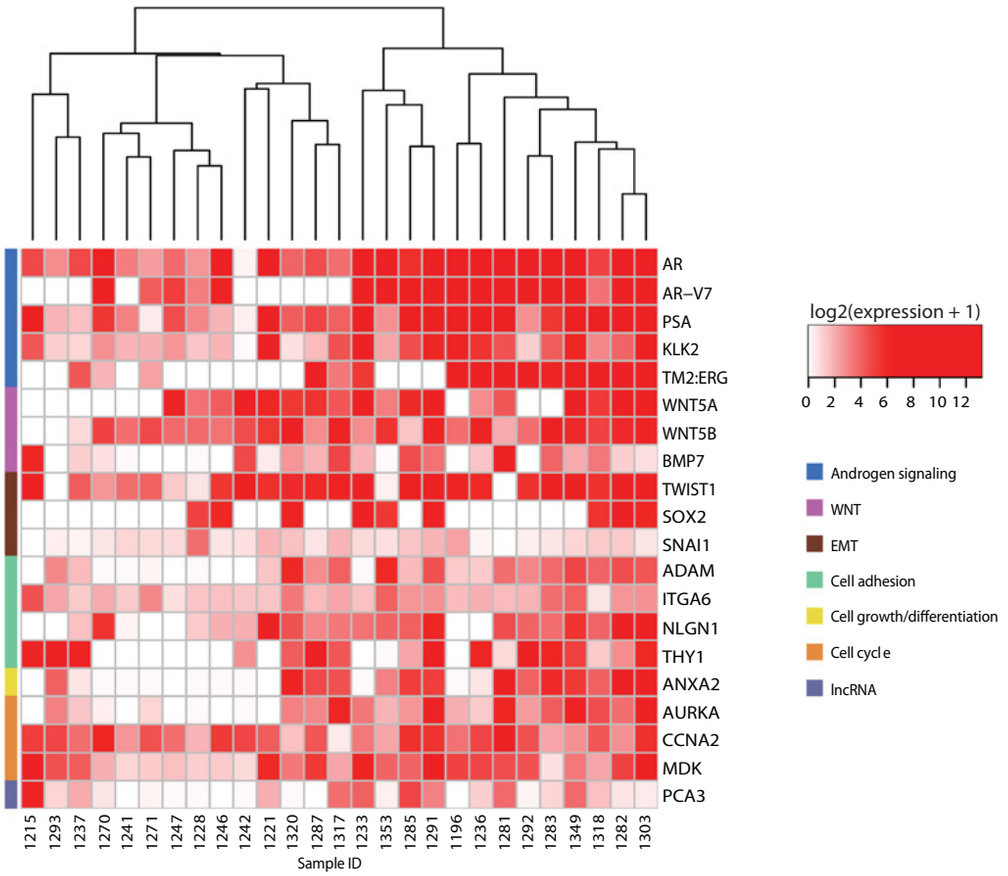

B

	Overall survival							
	Univariate analysis				Bivariate analysis			
Gene	HR	95% CI	*P*	FDR	HR	95% CI	*P*	FDR
Halabi score	1.43	(0.93–2.25)	0.1	-	-	-	-	-
WNT5a	3.59	(1.67–7.70)	0.001	0.06	3.62	(1.63–8.05)	0.002	0.08
BMP7	2.53	(1.15–5.57)	0.02	0.40	3.86	(1.60–9.32)	0.003	0.08
AUKRA	3.05	(1.10–8.44)	0.03	0.40	5.56	(1.79–17.20)	0.003	0.08
NLGN1	3.99	(1.70–9.37)	0.001	0.06	3.60	(1.41–9.21)	0.008	0.15
AR	3.34	(1.32–8.44)	0.01	0.28	3.37	(1.28–8.88)	0.01	0.19
ANXA2	2.81	(0.95–8.29)	0.06	0.40	4.25	(1.33–13.50)	0.01	0.19
ITGA6	1.81	(0.96–3.40)	0.06	0.40	2.32	(1.16–4.63)	0.01	0.19
ADAM	3.03	(0.93–9.89)	0.06	0.40	4.23	(1.22–14.60)	0.02	0.20
TWIST1	1.90	(1.02–3.54)	0.04	0.40	2.19	(1.11–4.31)	0.02	0.20
SOX2	1.83	(0.94–3.55)	0.07	0.42	1.98	(1.00–3.94)	0.05	0.40
PCA3	1.58	(0.83–3.00)	0.16	0.63	1.94	(0.97–3.89)	0.06	0.41
MDK	2.00	(0.91–4.37)	0.08	0.44	2.11	(0.96–4.65)	0.06	0.41
WNT5B	2.66	(1.04–6.76)	0.04	0.40	2.48	(0.93–6.63)	0.07	0.42
TM2:ERG	1.74	(0.69–4.41)	0.24	0.68	2.19	(0.87–5.48)	0.09	0.51
KLK2	2.21	(1.02–4.80)	0.04	0.40	1.96	(0.88–4.38)	0.09	0.51
PSA	2.36	(1.01–5.50)	0.04	0.40	2.07	(0.86–5.00)	0.10	0.51
THY1	1.30	(0.59–2.87)	0.51	0.87	2.17	(0.82–5.73)	0.11	0.54
SNAI1	0.71	(0.39–1.29)	0.25	0.68	0.53	(0.23–1.19)	0.12	0.54
CCNA2	1.61	(0.62–4.18)	0.32	0.77	2.13	(0.78–5.81)	0.14	0.56
ARV7	1.86	(0.65–5.30)	0.24	0.68	2.29	(0.75–6.99)	0.14	0.56

Figure 1.

CTC gene expression analysis reveals WNT5a, AURKA, and BMP7 are independently associated with overall survival in mCRPC. **A,** A heatmap representation of the top 20 independently predictive genes as determined by the Cox proportional hazards model. Each column represents a different sample and each row represents a separate gene. The heatmap color spectrum corresponds to lower relative expression (white) and higher relative expression (red). The left-colored column represents the associated functional pathway for each separate gene. **B,** WNT5a, BMP7, and AURKA (highlighted in blue) are independently associated with overall survival with $P < 0.05$ and FDR <10% when adjusting for Halabi variables.

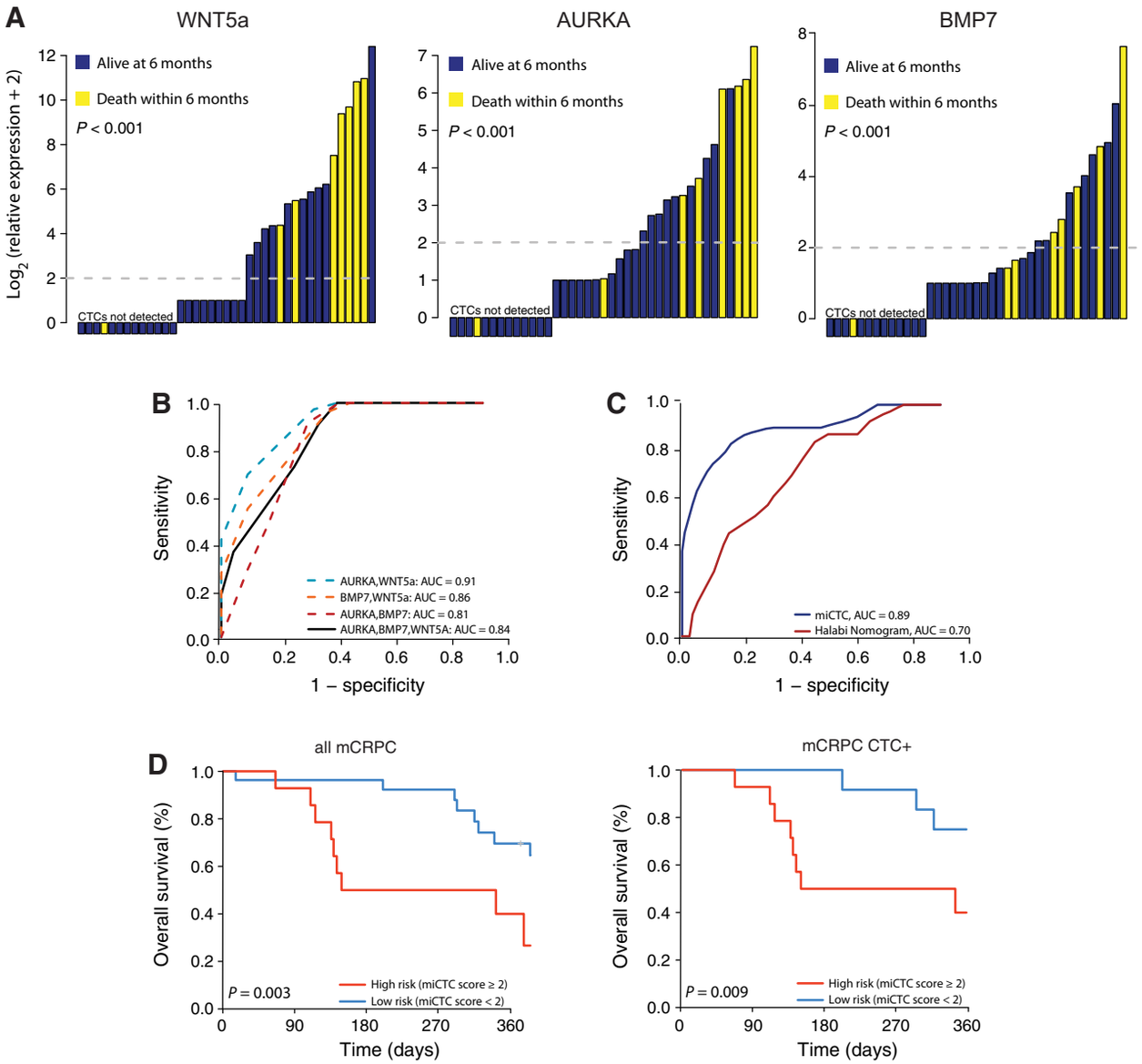

Figure 2.

A score combining Halabi, WNT5a, and AURKA improves prediction of overall survival at 6 months over Halabi alone. **A,** Survival status at 6 months based on normalized expression of WNT5a, AURKA, and BMP7 in 39 (26 CTC positive) patients with mCRPC. The hypergeometric distribution was used to test whether deaths were overrepresented in the top 25% of patients. Deaths were significantly overrepresented at the 1% level for all three genes ($P < 0.001$). **B,** Receiver operating characteristic (ROC) curve compares accuracy of WNT5a, AURKA, and BMP7 expression for predicting overall survival at 6 months. **C,** ROC curve compares accuracy of Halabi score alone (AUC = 0.70) vs. miCTC score (AUC = 0.89) combining Halabi score, WNT5a, and AURKA expression. **D,** Kaplan– Meier curves depicting overall survival in patients with high vs. low miCTC score. Left curve represents entire mCRPC patient cohort (CTC±), right curve represents only CTC-positive mCRPC patients.

with a greater risk of biochemical recurrence, metastasis, and death, and decreased prostate cancer-free survival when compared with those with lower-risk miCTC scores (Fig. 4A–D).

Discussion

Given the relative simplicity of obtaining single blood draws, CTCs obtained from whole blood may provide a compelling source of molecular information, and previous studies have shown that CTCs closely reflect the clinical and functional characteristics of solid tumors (57, 58). While the clinical significance of the presence of CTCs has long been theorized, improvements in the downstream manipulation and comprehensive molecular characterization of liquid biopsy tools are more recent. For example, a plasma-based real-time PCR test for the qualitative detection of defined mutations of the epidermal growth factor

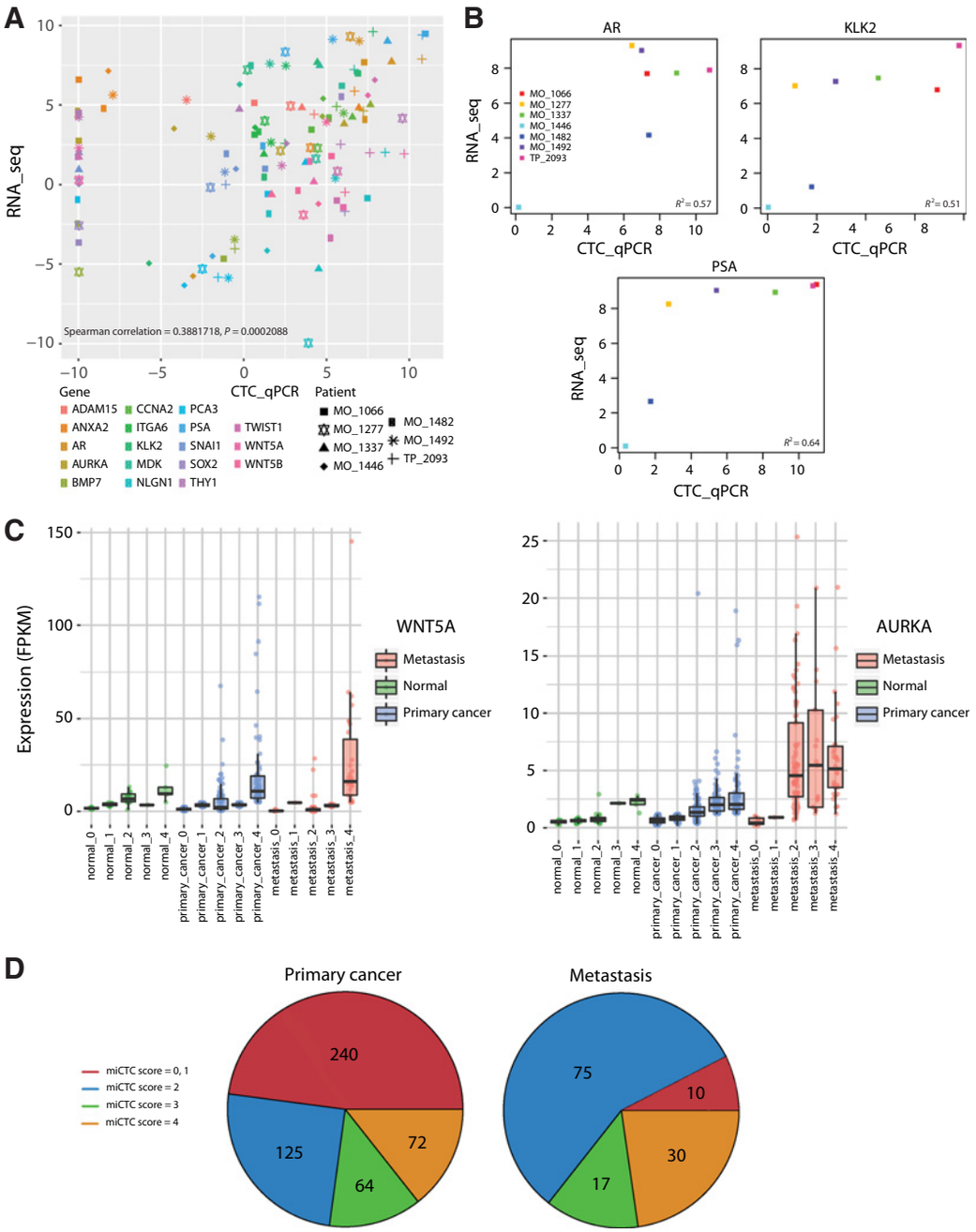

Figure 3.

Concordance of CTC gene expression by qPCR with known tissue-based RNA-seq expression. **A,** Global analysis of expression for select genes in CTCs of 7 patients after isolation and qPCR via platform with known RNA-seq data from MI-ONCOSEQ (Spearman correlation = 0.38, $P = 0.0002$); **B,** AR ($r^2 = 0.57$), KLK2 ($r^2 = 0.51$), and PSA ($r^2 = 0.64$) show concordance of expression between CTC qPCR and RNA-seq from MI-ONCOSEQ of 7 patients. **C,** Analysis of expression of AURKA and WNT5a by RNA-seq in an external cohort* (**D**) calculated miCTC score in external cohort of patients with primary and metastatic prostate cancer* (numbers within each pie represent number of samples with that specific miCTC score), *primary tumor samples obtained from TCGA, metastatic samples from SU2C.

receptor (*EGFR*) gene was recently developed to aid in the selection of non–small cell lung carcinoma (NSCLC) patients for treatment with erlotinib (59). The cobas EGFR Mutation Test, along with the CellSearch platform (50, 60, 61), currently represent the only FDA-approved liquid biopsy tests that may help guide first-line treatment decisions in patients, further underscoring the significant impact prospective cfDNA and CTC-based diagnostic and prognostic tools may have.

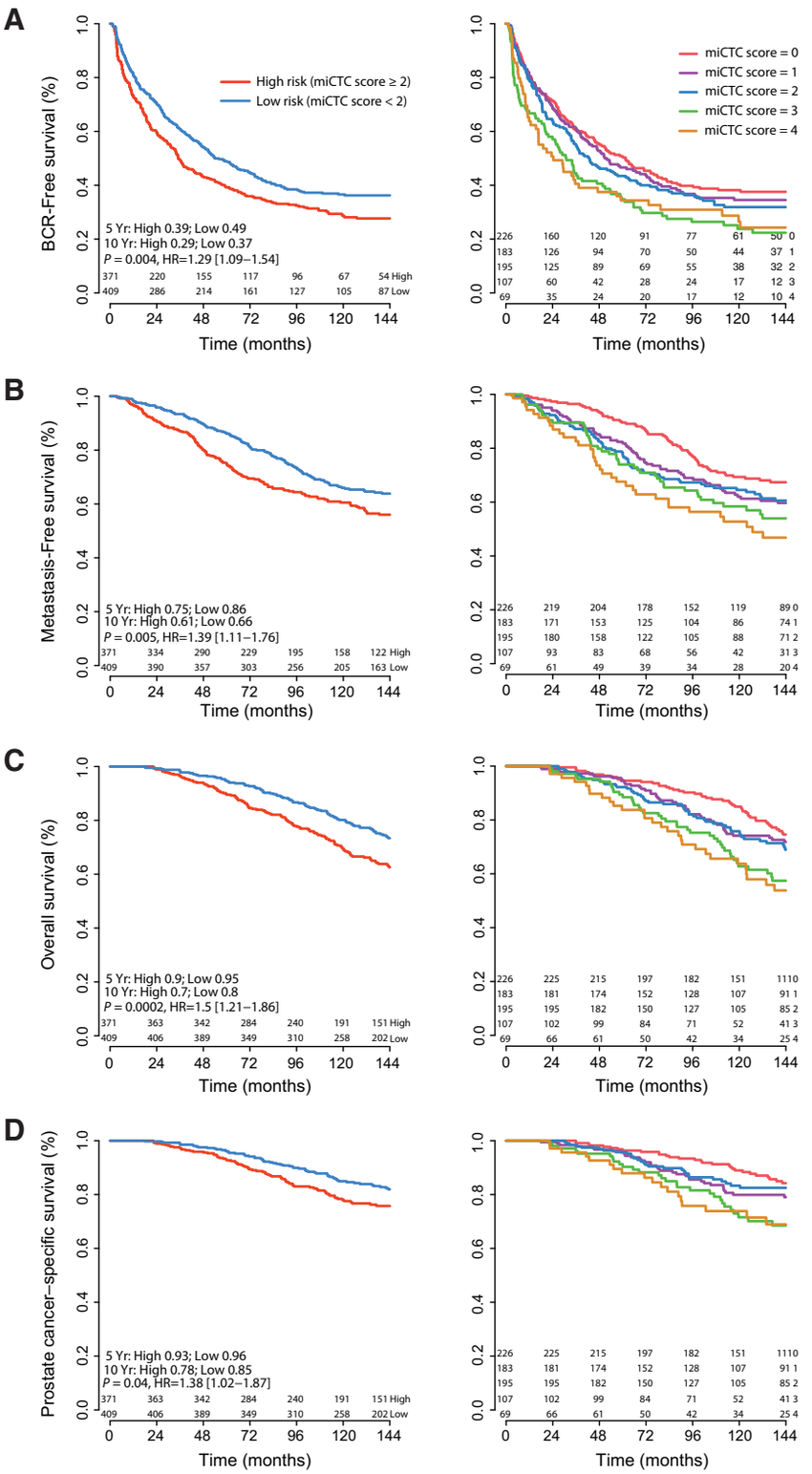

Figure 4.
miCTC score predicts long-term outcomes in patients with high-risk prostate cancer. Kaplan–Meier curves showing high risk (miCTC $\geq$2) and increasing miCTC score is associated with decreased; **A,** biochemical recurrence-free survival ($P = 0.004$); **B,** metastasis-free survival ($P = 0.005$); **C,** overall survival ($P = 0.002$); **D,** and prostate cancer–specific survival ($P = 0.04$) in high-risk, clinically localized prostate cancer (Mayo Clinic).

While *AR-V7* expression in CTCs has received a great deal of attention, we sought to develop a reproducible platform allowing CTC-based expression analysis across a broader panel of prostate cancer–related genes. This targeted approach was selected to improve the efficiency of the assay and potential clinical applicability, given the challenges inherent to CTC isolation and subsequent gene expression profiling. Although an unbiased approach would capture increased genetic

heterogeneity and support the discovery of novel gene targets, it would be increasingly difficult to differentiate possible prognostic targets from genetic noise, especially using a qPCR-based approach (62). Additionally, the likelihood of type 1 errors due to multiple testing is substantially greater with a broad, unbiased approach. Our primary goal was to utilize this platform to identify clinically relevant genes able to predict key oncologic outcomes in mCRPC.

In this cohort of mCRPC patients on a variety of therapies, *AR-V7* expression was not significantly associated with survival. However, a number of findings appeared to support the clinical validity of the approach utilized here. First, the expression data demonstrated a high degree of AR signaling in a majority of samples, with over half of samples showing AR splice variants. Second, we detected a global increase in prometastatic factors within CTCs, including genes involved in EMT, cell cycle regulation, and lncRNA-mediated tumor suppression (49, 52, 53, 63). Third, in patients with matched tissue-based gene expression available, there was a close correlation between the tissue and CTC-based results. Lastly, the tissue-based analysis in the localized disease setting provides evidence that the markers identified in our CTC-based approach also have applicability in earlier stage disease. While a "proof of concept" rather than a validation, the crude miCTC score based solely on expression was applied to clinical outcomes in prostatectomy patients as a preliminary analysis to further corroborate the prognostic relevance of the genes identified here.

Strikingly, our results add further support to the importance of noncanonical Wnt signaling as an alternative resistance pathway contributing to prostate cancer progression and worse clinical outcomes. While Wnt signaling has been previously linked to prostate cancer aggressiveness through various cellular functions (13, 14, 18, 64, 65), our data strongly corroborate another recent study linking Wnt signaling to antiandrogen resistance in CTCs (16). Additionally, Beltran and colleagues established the role of *AURKA* in prostate cancer proliferation and, in particular, in driving the development of neuroendocrine prostate cancer (NEPC). This has led to an ongoing phase II trial of aurora kinase A inhibition in NEPC (NCT01799278; refs. 4, 53). The miCTC score, driven by *WNT5a* and *AURKA* expression, reliably predicts overall survival in this development cohort, suggesting CTC genomics may mirror tissue-based drivers of variant or lethal prostate cancer.

The present study is limited by its relatively small sample size, and further prospective validation in larger cohorts will be required in order to confirm the clinical validity of these findings. Additionally, patients in this study were on a variety of therapies at the time of analysis. Evaluation of more homogenous cohorts is needed in order to ascertain the impact of specific therapeutic modalities on changes in gene expression over time and to develop predictive signatures of therapeutic response. However, the high event rate allowed us to identify several potential prognostic markers after adjusting for baseline clinical characteristics and determining false discovery rates.

While our CTC isolation protocol allows for simple, rapid processing of samples with high sensitivity, the approach itself has inherent limitations. Specifically, this protocol does not allow for CTC enumeration and no cell morphological assessment can be conducted. As a result, gene expression is not adjusted for number of CTCs and may be impacted by CTC quantity within a sample. However, the lack of correlation between epithelial score and survival indicates that CTC quantity itself is not a useful marker with this platform. Additionally, given that the platform is based on enrichment rather than isolation, gene expression analysis requires adjustment for background leukocyte contamination. Finally, as with other epithelial-based CTC detection approaches, the enrichment platform utilized here could miss CTCs that have undergone EMT and no longer express EpCaM on their cell surface (66).

These limitations notwithstanding, we developed a clinically relevant, multigene signature from CTCs using a scalable qPCR-based platform. Though external validation is needed, this molecular signature appears to strongly inform prognosis in patients with advanced prostate cancer. The strong prognostic performance of this signature in a tissue-based analysis of a large prostatectomy cohort further supports the potential clinical applicability of these data. We anticipate that this approach will facilitate serial patient assessments over time and identification of molecular changes as they occur in response to therapy. With continued improvement in the ability to determine key drivers of tumor progression using CTCs, we anticipate that this noninvasive, liquid-based approach will circumvent the need for invasive extraction of genomic material from bone metastases and guide precision medicine therapeutics in prostate cancer.

Disclosure of Potential Conflicts of Interest

R.J. Karnes reports receiving a commercial research grant from GenomeDx, has ownership interest (including patents) in GenomeDx, is a consultant/advisory board member for Genomic Health. S.L. Chang is a bioinformatician at PFS Genomics and has ownership interest in patents pending with GenomeDX Biosciences on genomic signatures unrelated to the work in this article. F.Y. Feng is a consultant/advisory board member for Janssen, Astellas/Medivation, Sanofi, Ferring, and Dendreon. S.A. Tomlins is Co-founder of, consultant for, and Laboratory Director for Strata Oncology, reports receiving a commercial research grants from Astellas/Medivation and GenomeDX, is a consultant/advisory board member for Astellas/Medivation, Janssen, Sanofi, and Almac Diagnostics and has received Travel Support from Thermo Fisher Scientific. No potential conflicts of interest were disclosed by the other authors.

Authors' Contributions

Conception and design: U. Singhal, Y. Wang, Y.S. Niknafs, Y. Qiao, R.S. Taichman, S.A. Tomlins, T.M. Morgan

Development of methodology: U. Singhal, Y. Wang, T.M. Morgan

Acquisition of data (provided animals, acquired and managed patients, provided facilities, etc.): U. Singhal, Y. Wang, Y. Qiao, A. Gursky, D.C. Smith, R.J. Karnes, F.Y. Feng, G.S. Palapattu, T.M. Morgan

Analysis and interpretation of data (e.g., statistical analysis, biostatistics, computational analysis): U. Singhal, Y. Wang, J. Henderson, Y.S. Niknafs, Y. Qiao, S.L.Chang, F.Y. Feng, G.S. Palapattu, A.M. Chinnaiyan, T.M. Morgan

Writing, review, and/or revision of the manuscript: U. Singhal, Y. Wang, J. Henderson, Y. Qiao, A. Zaslavsky, R.J. Karnes, S.L.Chang, F.Y. Feng, R.S. Taichman, A.M. Chinnaiyan, S.A. Tomlins, T.M. Morgan

Administrative, technical, or material support (i.e., reporting or organizing data, constructing databases): U. Singhal, Y. Wang, Y. Qiao, J.S. Chung, T.M. Morgan

Study supervision: U. Singhal, Y. Wang, G.S. Palapattu, T.M. Morgan

Acknowledgments

This study was supported by a Department of Defense Physician Research Training Award (W81XWH-14-1-0287) and the Prostate Cancer Foundation (T.M. Morgan, R.S. Taichman, and S.A. Tomlins). T.M. Morgan and S.A. Tomlins are also supported by the A. Alfred Taubman Medical Research Institute. This work was also supported by the NIH: National Cancer Institute PO1CA093900-10 and the University of Michigan Comprehensive Cancer Center Prostate SPORE (P50CA 069568).

The authors would like to thank Jun Luo, PhD, and Ken Pienta, MD, for assistance and mentorship in conducting this work. We also thank Robin Kunkel for help with figure preparation.

The costs of publication of this article were defrayed in part by the payment of page charges. This article must therefore be hereby marked *advertisement* in accordance with 18 U.S.C. Section 1734 solely to indicate this fact.

Received September 25, 2017; revised December 17, 2017; accepted February 6, 2018; published first February 16, 2018.

References

1. Siegel RL, Miller KD, Jemal A. Cancer statistics, 2016. CA Cancer J Clin 2016;66:7–30.
2. Pritchard CC, Mateo J, Walsh MF, De Sarkar N, Abida W, Beltran H, et al. Inherited DNA-repair gene mutations in men with metastatic prostate cancer. N Engl J Med 2016;375:443–53.
3. Qiao Y, Feng FY, Wang Y, Cao X, Han S, Wilder-Romans K, et al. Mechanistic support for combined MET and AR blockade in castration-resistant prostate cancer. Neoplasia 2016;18:1–9.
4. Beltran H, Prandi D, Mosquera JM, Benelli M, Puca L, Cyrta J, et al. Divergent clonal evolution of castration-resistant neuroendocrine prostate cancer. Nat Med 2016;22:298–305.
5. Grasso CS, Cani AK, Hovelson DH, Quist MJ, Douville NJ, Yadati V, et al. Integrative molecular profiling of routine clinical prostate cancer specimens. Ann Oncol 2015;26:1110–8.
6. Grasso CS, Wu YM, Robinson DR, Cao X, Dhanasekaran SM, Khan AP, et al. et al.The mutational landscape of lethal castration-resistant prostate cancer. Nature 2012;487:239–43.
7. Egan A, Dong Y, Zhang H, Qi Y, Balk SP, Sartor O. Castration-resistant prostate cancer: adaptive responses in the androgen axis. Cancer Treat Rev 2014;40:426–33.
8. Karantanos T, Corn PG, Thompson TC. Prostate cancer progression after androgen deprivation therapy: mechanisms of castrate resistance and novel therapeutic approaches. Oncogene 2013;32:5501–11.
9. Antonarakis ES, Lu C, Wang H, Luber B, Nakazawa M, Roeser JC, et al. AR-V7 and resistance to enzalutamide and abiraterone in prostate cancer. N Engl J Med 2014;371:1028–38.
10. Harris WP, Mostaghel EA, Nelson PS, Montgomery B. Androgen deprivation therapy: progress in understanding mechanisms of resistance and optimizing androgen depletion. Nat Clin Pract Urol 2009;6:76–85.
11. Taplin ME, Bubley GJ, Shuster TD, Frantz ME, Spooner AE, Ogata GK, et al. Mutation of the androgen-receptor gene in metastatic androgen-independent prostate cancer. N Engl J Med 1995;332:1393–8.
12. Yokoyama NN, Shao S, Hoang BH, Mercola D, Zi X. Wnt signaling in castration-resistant prostate cancer: implications for therapy. Am J Clin Exp Urol 2014;2:27–44.
13. Takahashi S, Watanabe T, Okada M, Inoue K, Ueda T, Takada I, et al. Noncanonical Wnt signaling mediates androgen-dependent tumor growth in a mouse model of prostate cancer. Proc Natl Acad Sci U S A 2011;108:4938–43.
14. Zheng D, Decker KF, Zhou T, Chen J, Qi Z, Jacobs K, et al. Role of WNT7B-induced noncanonical pathway in advanced prostate cancer. Mol Cancer Res 2013;11:482–93.
15. Bisson I, Prowse DM. WNT signaling regulates self-renewal and differentiation of prostate cancer cells with stem cell characteristics. Cell Res 2009;19:683–97.
16. Miyamoto DT, Zheng Y, Wittner BS, Lee RJ, Zhu H, Broderick KT, et al. RNA-Seq of single prostate CTCs implicates noncanonical Wnt signaling in antiandrogen resistance. Science 2015;349:1351–6.
17. Gerlinger M, Rowan AJ, Horswell S, Math M, Larkin J, Endesfelder D, et al. Intratumor heterogeneity and branched evolution revealed by multiregion sequencing. N Engl J Med 2012;366:883–92.
18. Robinson D, Van Allen Eliezer M, Wu YM, Schultz N, Lonigro RJ, Mosquera JM, et al. Integrative clinical genomics of advanced prostate cancer. Cell 2015;161:1215–28.
19. Kumar A, Coleman I, Morrissey C, Zhang X, True LD, Gulati R, et al. Substantial interindividual and limited intraindividual genomic diversity among tumors from men with metastatic prostate cancer. Nat Med 2016;22:369–78.
20. Scher HI, Morris MJ, Larson S, Heller G. Validation and clinical utility of prostate cancer biomarkers. Nat Rev Clin Oncol 2013;10:225–34.
21. Stott SL, Lee RJ, Nagrath S, Yu M, Miyamoto DT, Ulkus L, et al. Isolation and characterization of circulating tumor cells from patients with localized and metastatic prostate cancer. Sci Transl Med 2010;2:25ra23.
22. Aceto N, Bardia A, Miyamoto DT, Donaldson MC, Wittner BS, Spencer JA, et al. Circulating tumor cell clusters are oligoclonal precursors of breast cancer metastasis. Cell 2014;158:1110–22.
23. Danila DC, Heller G, Gignac GA, Gonzalez-Espinoza R, Anand A, Tanaka E, et al. Circulating tumor cell number and prognosis in progressive castration-resistant prostate cancer. Clin Cancer Res 2007;13:7053–8.
24. Scher HI, Jia X, de Bono JS, Fleisher M, Pienta KJ, Raghavan D, et al. Circulating tumour cells as prognostic markers in progressive, castration-resistant prostate cancer: a reanalysis of IMMC38 trial data. Lancet Oncol 2009;10:233–9.
25. Shaffer DR, Leversha MA, Danila DC, Lin O, Gonzalez-Espinoza R, Gu B, et al. Circulating tumor cell analysis in patients with progressive castration-resistant prostate cancer. Clin Cancer Res 2007;13:2023–9.
26. Vogelzang NJ, Fizazi K, Burke JM, De Wit R, Bellmunt J, Hutson TE, et al. Circulating tumor cells in a phase 3 study of docetaxel and prednisone with or without lenalidomide in metastatic castration-resistant prostate cancer. Eur Urol 2017;71:168–71.
27. Wyatt AW, Azad AA, Volik SV, Annala M, Beja K, McConeghy B, et al. Genomic alterations in cell-free DNA and enzalutamide resistance in castration-resistant prostate cancer. JAMA Oncol 2016;2:1598–606.
28. Schwarzenbach H, Alix-Panabières C, Müller I, Letang N, Vendrell JP, Rebillard X, et al. Cell-free tumor DNA in blood plasma as a marker for circulating tumor cells in prostate cancer. Clin Cancer Res 2009;15:1032.
29. Yu M, Stott S, Toner M, Maheswaran S, Haber DA. Circulating tumor cells: approaches to isolation and characterization. J Cell Biol 2011;192:373–82.
30. Ozkumur E, Shah AM, Ciciliano JC, Emmink BL, Miyamoto DT, Brachtel E, et al. Inertial focusing for tumor antigen–dependent and –independent sorting of rare circulating tumor cells. Sci Transl Med 2013;5:179ra47.
31. Cuzick J, Swanson GP, Fisher G, Brothman AR, Berney DM, Reid JE, et al. Prognostic value of an RNA expression signature derived from cell cycle proliferation genes in patients with prostate cancer: a retrospective study. Lancet Oncol 2011;12:245–55.
32. Knezevic D, Goddard AD, Natraj N, Cherbavaz DB, Clark-Langone KM, Snable J, et al. Analytical validation of the Oncotype DX prostate cancer assay – a clinical RT-PCR assay optimized for prostate needle biopsies. BMC Genomics 2013;14:690.
33. Mehlen P, Puisieux A. Metastasis: a question of life or death. Nat Rev Cancer 2006;6:449–58.
34. Schmittgen TD, Livak KJ. Analyzing real-time PCR data by the comparative C(T) method. Nat Protoc 2008;3:1101–8.
35. David CR. Regression models and life tables (with discussion). J Roy Statist Soc Ser A 1972;34:187–220.
36. Therneau T. A package for survival analysis in S. R package version 2.37-4. Available from: https://cran.r-project.org/.
37. Benjamini Y, Hochberg Y. Controlling the false discovery rate: a practical and powerful approach to multiple testing. J R Stat Soc Series B Methodol 1995;57:289–300.
38. Heagerty PJ, Lumley T, Pepe MS. Timedependent ROC curves for censored survival data and a diagnostic marker. Biometrics 2000;56:337–44.
39. Heagerty P, Saha P. SurvivalROC: time-dependent ROC curve estimation from censored survival data. Biometrics 2000;56:337–44.
40. R Core Team (2014). R: A language and environment for statistical computing. R Foundation for Statistical Computing, Vienna, Austria. Available from; http://www.R-project.org/.
41. Erho N, Crisan A, Vergara IA, Mitra AP, Ghadessi M, Buerki C, et al. Discovery and validation of a prostate cancer genomic classifier that

predicts early metastasis following radical prostatectomy. PLoS One 2013; 8:e66855.
42. Karnes RJ, Bergstralh EJ, Davicioni E, Ghadessi M, Buerki C, Mitra AP, et al. Validation of a genomic classifier that predicts metastasis following radical prostatectomy in an at risk patient population. J Urol 2013;190:2047–53.
43. Nakagawa T, Kollmeyer TM, Morlan BW, Anderson SK, Bergstralh EJ, Davis BJ, et al. A tissue biomarker panel predicting systemic progression after PSA recurrence post-definitive prostate cancer therapy. PLoS One 2008;3:e2318.
44. Piccolo SR, Sun Y, Campbell JD, Lenburg ME, Bild AH, Johnson WE. A single-sample microarray normalization method to facilitate personalized-medicine workflows. Genomics 2012;100:337–44.
45. Tomlins SA, Rhodes DR, Perner S, Dhanasekaran SM, Mehra R, Sun XW, et al. Recurrent fusion of TMPRSS2 and ETS transcription factor genes in prostate cancer. Science 2005;310:644–8.
46. Grossmann ME, Huang H, Tindall DJ. Androgen receptor signaling in androgen-refractory prostate cancer. J Natl Cancer Inst 2001;93:1687–97.
47. Bhatia-Gaur R, Donjacour AA, Sciavolino PJ, Kim M, Desai N, Young P, et al. Roles for Nkx3.1 in prostate development and cancer. Genes Dev 1999;13:966–77.
48. Traish AM, Morgentaler A. Epidermal growth factor receptor expression escapes androgen regulation in prostate cancer: a potential molecular switch for tumour growth. Br J Cancer 2009;101:1949–56.
49. Prensner JR, Iyer MK, Sahu A, Asangani IA, Cao Q, Patel L, et al. The long noncoding RNA SChLAP1 promotes aggressive prostate cancer and antagonizes the SWI/SNF complex. Nat Genet 2013;45:1392–8.
50. Kagan M, Howard D, Bendele T, et al. Circulating tumor cells as cancer markers, a sample preparation and analysis system. In: Diamandis EP, Fritsche HA, Lilja H, Chan DW, Schwartz M, editors. Tumor markers: physiology, pathobiology, technology and clinical applications. Washington, DC: AACC Press; 2002; pp. 495–8.
51. Halabi S, Lin CY, Kelly WK, Fizazi KS, Moul JW, Kaplan EB, et al. Updated prognostic model for predicting overall survival in first-line chemotherapy for patients with metastatic castration-resistant prostate cancer. J Clin Oncol 2014;32:671–7.
52. Aparicio A, Logothetis CJ, Maity SN. Understanding the lethal variant of prostate cancer: power of examining extremes. Cancer Discov 2011;1:466–8.
53. Beltran H, Rickman DS, Park K, Chae SS, Sboner A, MacDonald TY, et al. Molecular characterization of neuroendocrine prostate cancer and identification of new drug targets. Cancer Discov 2011;1:487–95.
54. Morrissey C, Brown LG, Pitts TE, Vessella RL, Corey E. Bone morphogenetic protein 7 is expressed in prostate cancer metastases and its effects on prostate tumor cells depend on cell phenotype and the tumor microenvironment. Neoplasia 2010;12:192–205.
55. Roychowdhury S, Iyer MK, Robinson DR, Lonigro RJ, Wu YM, Cao X, et al. Personalized oncology through integrative high-throughput sequencing: a pilot study. Sci Transl Med 2011;3:111ra121.
56. Cancer Genome Atlas Research N. The molecular taxonomy of primary prostate cancer. Cell 2015;163:1011–25.
57. Yu M, Bardia A, Aceto N, Bersani F, Madden MW, Donaldson MC, et al. Ex vivo culture of circulating breast tumor cells for individualized testing of drug susceptibility. Science 2014;345:216–20.
58. Mishima Y, Paiva B, Shi J, Park J, Manier S, Takagi S, et al. The mutational landscape of circulating tumor cells in multiple myeloma. Cell Rep 2017;19:218–24.
59. Wu YL, Zhou C, Liam CK, Wu G, Liu X, Zhong Z, et al. First-line erlotinib versus gemcitabine/cisplatin in patients with advanced EGFR mutation-positive non-small-cell lung cancer: analyses from the phase III, randomized, open-label, ENSURE study. Ann Oncol 2015;26:1883–9.
60. Cristofanilli M, Budd GT, Ellis MJ, Stopeck A, Matera J, Miller MC, et al. Circulating tumor cells, disease progression, and survival in metastatic breast cancer. N Engl J Med 2004;351:781–91.
61. Cristofanilli M, Hayes DF, Budd GT, Ellis MJ, Stopeck A, Reuben JM, et al. Circulating tumor cells: a novel prognostic factor for newly diagnosed metastatic breast cancer. J Clin Oncol 2005;23:1420–30.
62. Bianchi F, Nicassio F, Di Fiore PP. Unbiased vs. biased approaches to the identification of cancer signatures: the case of lung cancer. Cell Cycle 2008;7:729–34.
63. Mego M, Mani SA, Cristofanilli M. Molecular mechanisms of metastasis in breast cancer—clinical applications. Nat Rev Clin Oncol 2010;7: 693–701.
64. Katoh M, Katoh M. WNT signaling pathway and stem cell signaling network. Clin Cancer Res 2007;13:4042–45.
65. Gujral TS, Chan M, Peshkin L, Sorger PK, Kirschner MW, MacBeath G. A noncanonical Frizzled2 pathway regulates epithelial-mesenchymal transition and metastasis. Cell 2014;159:844–56.
66. McDaniel AS, Ferraldeschi R, Krupa R, Landers M, Graf R, Louw J, et al. Phenotypic diversity of circulating tumour cells in patients with metastatic castration-resistant prostate cancer. BJU Int 2017;120:E30–44.